# Control of box C/D snoRNP assembly by N6-methylation of adenine

Huang, Lin; Ashraf, Saira; Wang, Jia; Lilley, David M. J.

*Published in:*
EMBO Reports

*DOI:*
10.15252/embr.201743967

*Publication date:*
2017

Published online: June 16, 2017

Article

OPEN ACCESS

EMBO reports

# Control of box C/D snoRNP assembly by $N^6$-methylation of adenine

Lin Huang, Saira Ashraf, Jia Wang & David MJ Lilley*

## Abstract

**$N^6$-methyladenine is the most widespread mRNA modification. A subset of human box C/D snoRNA species have target GAC sequences that lead to formation of $N^6$-methyladenine at a key *trans* Hoogsteen-sugar A·G base pair, of which half are methylated *in vivo*. The GAC target is conserved only in those that are methylated. Methylation prevents binding of the 15.5-kDa protein and the induced folding of the RNA. Thus, the assembly of the box C/D snoRNP could in principle be regulated by RNA methylation at its critical first stage. Crystallography reveals that $N^6$-methylation of adenine prevents the formation of *trans* Hoogsteen-sugar A·G base pairs, explaining why the box C/D RNA cannot adopt its kinked conformation. More generally, our data indicate that sheared A·G base pairs (but not Watson–Crick base pairs) are more susceptible to disruption by $N^6$mA methylation and are therefore possible regulatory sites. The human signal recognition particle RNA and many related Alu retrotransposon RNA species are also methylated at N6 of an adenine that forms a sheared base pair with guanine and mediates a key tertiary interaction.**

**Keywords** epigenetics; G·A base pairs; k-turn; RNA methylation; signal recognition particle

**Subject Categories** RNA Biology; Structural Biology

**DOI** 10.15252/embr.201743967 | Received 20 January 2017 | Revised 21 May 2017 | Accepted 22 May 2017

## Introduction

All cellular RNA is subject to dynamic covalent modification, and posttranscriptional modification of RNA is diverse and widespread [1,2]. $N^6$-methyladenine is the most common modification in RNA [3–5]. It is found in mRNA (a typical eukaryotic mRNA will have several such methylated adenine nucleotides), as well as in lncRNA species such as Xist [4,5] and MALAT1 [6,7]) and in viral RNA [8]. This epigenetic marker has proposed roles in the modulation of RNA stability [9], control of translation efficiency [10,11], and in gene regulation [12], and $N^6$-methyladenine is most frequently observed in regions of mRNA indicative of control functions [5]. The level of modification is subject to regulation by methyl transferase [13] and demethylase [14,15] enzymes, and they have been linked to human disease [15–18].

In this work, we have uncovered a putative role of epigenetic regulation in a subset of human snoRNP complexes that are involved in the site-specific modification of RNA. In archaea and the eukaryotes, the box C/D snoRNP complexes direct the site-specific 2′-*O*-methylation of rRNA and tRNA by providing complementary guide RNA for specificity and a SAM-dependent methyl transferase enzyme to modify the target ribose [19–26]. The complex is equivalent to a bulged RNA duplex, where both 12 nucleotide strands of the central region are the guide sequences that hybridize to the target RNA molecules to be methylated (Fig 1A). The conserved box C/D and C'/D' sequences are located in the duplexes that flank the guide region, and both adopt the k-turn conformation (k-turn structure is reviewed in [27]). A series of proteins assembles on the snoRNA [28–32]. In the first step, a member of the L7Ae family, the 15.5-kDa protein (15.5k) in humans, binds to each of the k-turns. This is followed by a Nop58 binding to box C/D and Nop56 binding to box C'/D', associating through a coiled-coil domain to form a heterodimer. Finally, two molecules of the methyl transferase fibrillarin associate with the complex to generate the catalytically active snoRNP. Thus, the key event that initiates the assembly of the complex is the association between the 15.5-kDa protein and the k-turn. In particular, Watkins *et al* [30] showed that if the binding of 15.5k to the human box C/D k-turn is prevented by sequence changes that are known to disrupt k-turn folding, this blocks assembly of the box C/D snoRNP.

Binding of L7Ae-family proteins induces the formation of the tightly kinked k-turn structure [33–35] (Fig 1B). The core of the k-turn structures formed by the box C/D and C'/D' elements comprises consecutive *trans* sugar-Hoogsteen G·A base pairs (sometimes termed sheared base pairs) that position the conserved adenine nucleobases to make key cross-strand hydrogen bonds that stabilize the conformation (Fig 1C). In general, k-turns fall into two classes depending on whether or not they will fold in response to the presence of metal ions [36]. We have noted that box C/D k-turns remain unfolded under these conditions, and so require protein-induced folding. Once this has been achieved the assembly of the snoRNP can proceed to form the active methylation complex. However, a process that blocks the folding of the k-turn would likely prevent the assembly of a functional snoRNP complex.

While the majority of k-turn structures have a C-G base pair at the -1b,-1n position, we have noted that in the box C/D k-turn

Cancer Research UK Nucleic Acid Structure Research Group, The University of Dundee, Dundee, UK
*Corresponding author. Tel: +44 1382 384243; E-mail: d.m.j.lilley@dundee.ac.uk

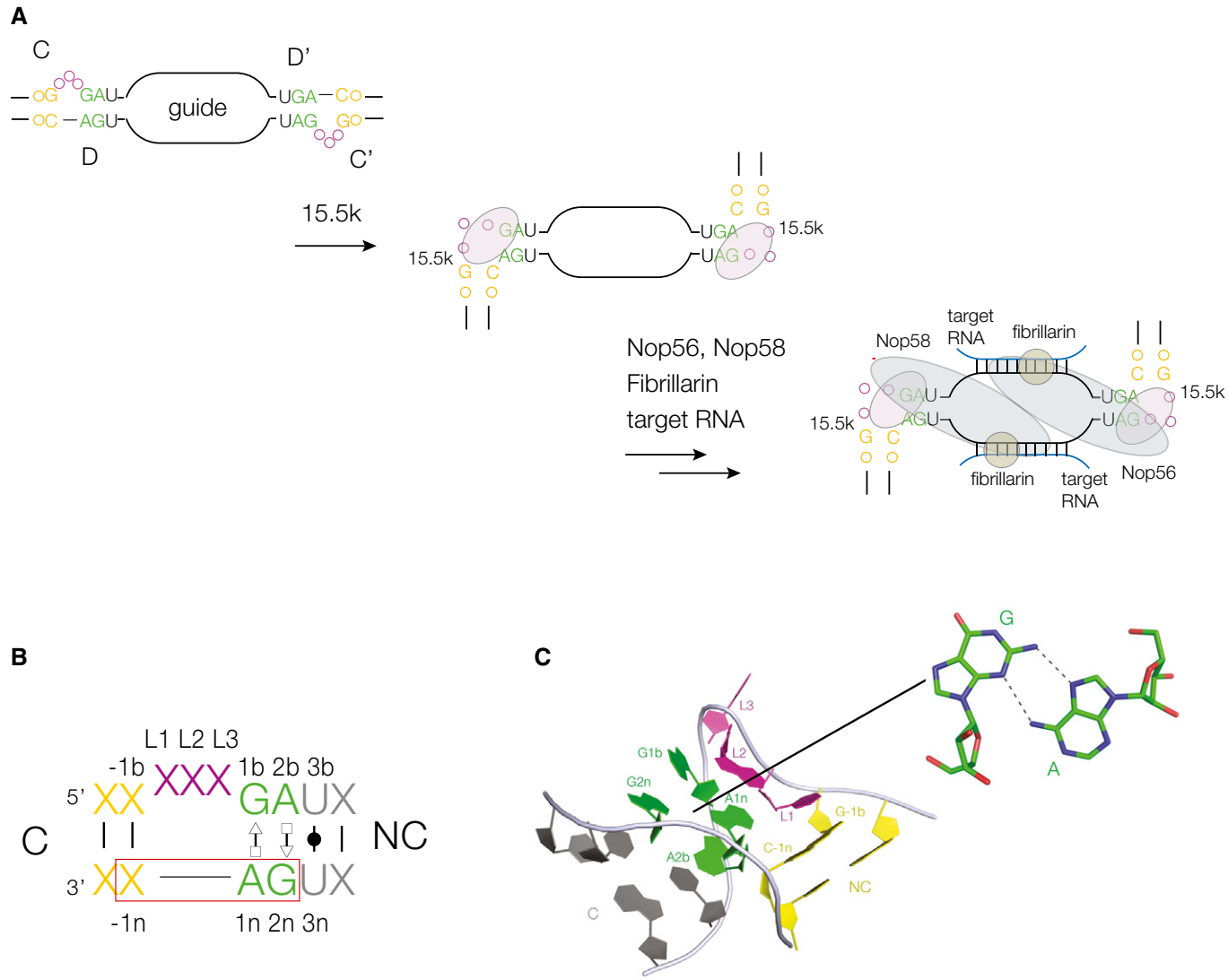


**Figure 1. Assembly of box C/D snoRNA, and their k-turn structures.**

A Scheme depicting the assembly of box C/D snoRNP. The first stage is the binding of the 15.5k protein to the box C/D and C'/D' k-turns.

B The general sequence of a k-turn, with the standard nomenclature of nucleotide positions. Note that when the -1n nucleotide is cytosine, this generates a GAC sequence on the non-bulged strand (boxed) that is a potential target for N$^6$-methylation of the conserved adenine at the 1n position. The two helical arms of the k-turn are named C (canonical) and NC (non-canonical) as indicated.

C Structure of a standard box C/D k-turn, together with the chemical structure of the G1b·A1n and A2b·G2n *trans* sugar-Hoogsteen G·A base pairs (PDB 1RLG [74]).

sequences this base pair is sometimes inverted, so that the -1n nucleotide is a cytosine. Since the highly conserved core of the k-turn requires 2n = G and 1n = A, this creates a GAC sequence on the non-bulged strand (boxed in Fig 1B) that is a putative target for methylation of adenine N6 [9]. Given the critical role of the A1n nucleobase in the folded k-turn, it seemed highly probable that N$^6$-methylation would interfere with folding. We have therefore studied the occurrence of -1n = C in human box C/D and C'/D' sequences. We find that a significant subset have -1n = C, about half of which are known to be methylated, and that those that are methylated are strongly conserved. We further show here that N$^6$-methyladenine at the 1n position of box C/D and C'/D' k-turns prevents specific binding of the 15.5k protein, and consequent induced folding, and use X-ray crystallography to provide a structural explanation for this. Indeed, our structural analysis indicates that sheared A·G base pairs are much more sensitive to N$^6$-methylation of adenine compared to Watson–Crick base pairs, and we show that these effects extend to other structures involving such A·G base pairs.

## Results

### N$^6$-adenine methylation of box C/D sequences

Analysis of the targets for methylation by the METTL3–METTL14 methyl transferase complex in eukaryotes shows the preferred

 

sequence to be DRACH (where D denotes A, G, or U; R is A or G; and H is A, C, or U), with GAC as the most common site of methylation [4,5]. The box C/D and C'/D' sequences adopt the k-turn conformation on binding the 15.5-kDa protein (15.5k), with the unbulged strand having GA at the 2n,1n sequence. In most other k-turns, the -1n nucleotide is G, but in some box C/D-type k-turns it is C, thus creating a GAC sequence with the central adenine as a potential methylation target (Fig 2A). N$^6$-methylation of the A1n might be anticipated to affect the folding of the k-turn into the kinked conformation. We therefore analyzed the occurrence of -1n = C in human box C/D and C'/D' sequences (although many D' boxes could not be reliably annotated either because of the short length of these snoRNA-like genes, or the lack of evolutionary conservation or sequence motif signals).

Using the snoRNABase [37] and snOPY [38] databases, we identified 27 human snoRNA sequences with 2n = G, 1n = A, and -1n = C, comprising 17 box D and 10 box D'. These are potential methylation targets, so we then examined the RMBase database [39], which contains single-nucleotide or high-resolution data on N$^6$-methyladenine sites [40,41], to see whether any had been experimentally demonstrated to be methylated *in vivo*. From this, we identified 14 human sequences that were shown to be N$^6$-methylated at A1n (eight from box D and six from box D') (Table 1, Fig 3). Most of these have been identified in more than one independent experiment. The A1n of SNORD13 from chromosome 8 was found to be methylated in 11 different sequencing experiments. Paralogs of SNORD13 and SNORD46 encoded on different chromosomal locations were found to be methylated.

If the N$^6$-methylation of A1n in these k-turn-forming snoRNA species is functionally significant then we might expect that the -1n = C sequence that is required to generate the methylation target should be conserved in other eukaryotes. We therefore examined the conservation of the -1n position in other organisms using the snoRNABase and snOPY databases (Appendix Table S1). We found that the -1n sequence is highly conserved as C for those 14 sequences that are methylated *in vivo*. This is 100% conserved in SNORD71 and SNORD101. 26 SNORD71 sequences are conserved in vertebrates including human, rat, chicken, frog, and fugu (pufferfish). Outside the conserved C, D, C', D' and guide region, only the -1n C and its complementary paired base (-1b = G) are 100% conserved (Fig 2B). In marked contrast, for 12 of 13 box C/D RNAs that are not methylated -1n is significantly less conserved as C. This is shown graphically in Fig 2C. Evidently, the -1n position of the snoRNA k-turn is critical for function in the methylated sequences, but much less so in those that are not.

### N$^6$-methylation of adenine 1n interferes with 15.5k-induced folding of box C/D and C'/D' k-turns

We have seen that in a subset of human box C/D k-turn sequences the -1n position is a cytosine, creating a GAC methylation target on the non-bulged strand. The METTL3-METTL14 methyl transferase complex could therefore convert the A1n of the k-turn to N$^6$-methyladenine. We know that k-turn folding is most sensitive to modification of the G1b·A1n base pair, and we therefore set out to test whether or not N$^6$-methyladenine would impair folding of box C/D-type k-turns. In general, these k-turn have sequences that are not susceptible to ion-induced folding [36] so that they require the binding of protein to undergo folding into the kinked conformation. For the human snoRNA species this is the 15.5k protein. We examined the folding of representative human box C/D and C'/D' k-turns in response to addition of human 15.5k using two approaches. One was by electrophoretic migration in non-denaturing polyacrylamide gels, where protein binding results in retardation of the RNA. The other is a spectroscopic method based upon fluorescence resonance energy transfer (FRET) between fluorescein and Cy3 fluorophores attached to the termini of a short snoRNA duplex with a central k-turn motif; protein-induced folding into the kinked conformation brings the fluorophores closer together, resulting in an increased efficiency of energy transfer ($E_{FRET}$).

Results are shown for one box C/D k-turn from SNORD13 (U13) snoRNA, and one box C'/D' k-turn from SNORD62A (U62A) snoRNA (Fig 4). The unmethylated RNA species both migrate as a discrete band of retarded mobility when incubated with either human 15.5k or *Archeoglobus fulgidus* L7Ae (*Af* L7Ae) protein (Fig 4A and C). At higher 15.5k concentrations, further retarded species are observed as a smear running up the gel, indicative of additional non-specific binding. Over the same range of 15.5k protein concentration used in the electrophoresis, the fluorescence spectroscopy reveals an increase in energy transfer (final $E_{FRET}$ = 0.6) indicative of a folding of the k-turns (Fig 4B and D). The affinity of *Af* L7Ae for a standard k-turn has been measured in the pM range [42], so it is expected that we observe stoichiometric binding in these experiments, and consequently, we cannot measure a dissociation constant for this class of protein. However, collectively these data indicate that the 15.5k protein binds to and induces the folding of the box C/D and box C'/D' k-turns.

By contrast, the corresponding RNA species with N$^6$-methyladenine at the 1n position exhibited very different behavior. Methylated versions of both U13 and U62A RNA failed to form discrete retarded complexes observed by gel electrophoresis (Fig 4A and C), rather forming smears up the gels at high 15.5k concentrations, indicative of non-specific binding. The fluorescence data (Fig 4B and D) show evidence of structural transitions at higher 15.5k concentration, with a significantly lower endpoint (final $E_{FRET}$ = 0.3) compared to the unmethylated RNA. Moreover, the shape of the transition indicates rather greater cooperativity. These results suggest non-specific binding of multiple protein molecules that fails to fold the methylated RNA into a normal k-turn conformation.

We have explored the binding of 15.5k protein to SNORD62A (U62A) snoRNA with and without N6 methylation of A1n using isothermal titration calorimetry (Appendix Fig S1). Binding results in the evolution of heat in an exothermic reaction for both species, and the fitted thermodynamic data are tabulated in Appendix Table S2. The titration of the unmethylated RNA is consistent with stoichiometric binding as anticipated, with close to 1:1 15.5k:RNA ratio in an enthalpically driven binding reaction. However, the character of the binding to the N$^6$A-methylated RNA is different, having lower values of $\Delta H$ and $T\Delta S$ and weaker apparent binding affinity, with a consequently different 15.5k protein–RNA ratio. This clearly reflects a significantly different protein binding mode between unmethylated and N$^6$A-methylated RNA, consistent with the results of the electrophoretic and FRET analysis, and confirming non-specific binding when the snoRNA is methylated.

Evidently, N$^6$-methylation of A1n disrupts the proper binding and folding of box C/D and C'/D' k-turns by the human 15.5k protein.

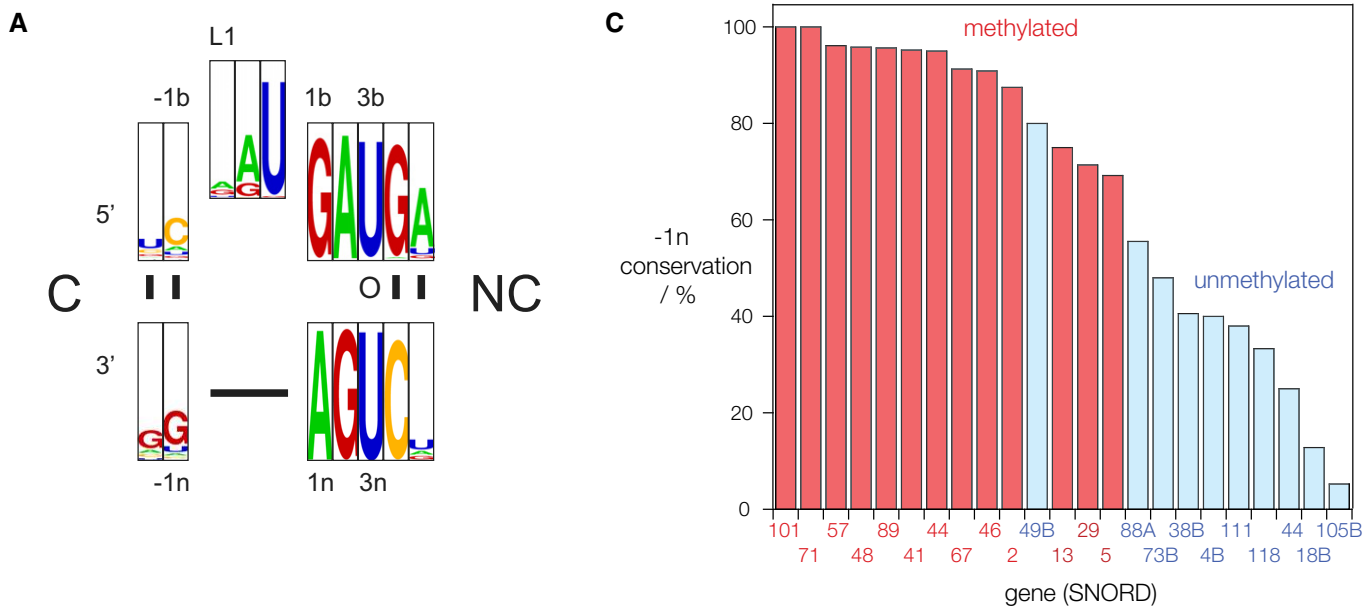


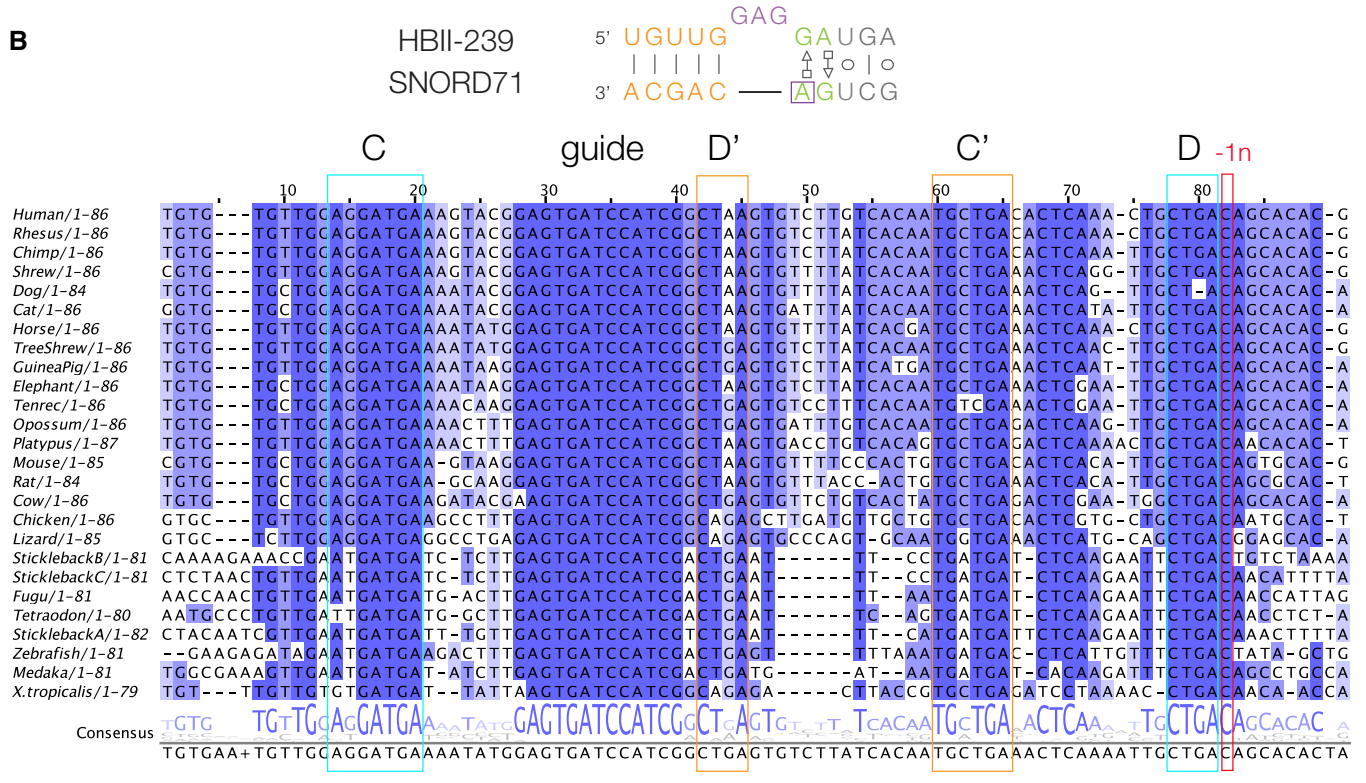


**Figure 2. Bioinformatic analysis of box C/D and C'/D' methylation in the human genome.**

A WebLogo plot showing the occurrence of box C/D sequences in human snoRNA. The frequency of distribution for the -1b,-1n pair is CG 65.27%; AU 8.78%; UA 4.96%; UG 4.20%; GC 3.82%.

B Sequence alignment for SNORD71. The boxes C, D, C', and D' are boxed, as is the -1n sequence.

C The conservation of -1n sequences (fraction of cytosine as percent) for eukaryotic box C/D and C'/D' sequences for which -1n = C in humans. Those that are methylated in humans are colored red while those that are not are colored blue.

### A structural basis for the effect of m$^6$A on k-turn folding

In order to understand the structural basis for the effect of N$^6$-methyladenine on k-turn conformation, we have used X-ray crystallography to investigate the structural effect of this modification on different base pairs involving adenine. Each species was formed by the hybridization of a self-complementary strand that contains a 5-bromocytosine nucleotide used to calculate phases for

 

**Table 1. BoxC/D RNA A1n N$^6$-methylation sites identified from RMBase. In human, 19 unique positions been modified, comprising 14 unique boxC/D RNA (8 D box and 6 D' box). In mouse, one D' box was identified; importantly, this site is also modified in humans.**

| Human | GeneName | modID | Chromosome | Position | Strand | SupportNum | Position in k-turn |
|---|---|---|---|---|---|---|---|
| 1 | SNORD13 | m6A_site_124853 | chr8 | 33371093 | + | 11 | boxD 1n |
| | SNORD13 | m6A_site_136193 | chrX | 23525329 | – | 8 | boxD 1n |
| | SNORD13 | m6A_site_24525 | chr11 | 66988484 | + | 3 | boxD 1n |
| | SNORD13 | m6A_site_130577 | chr9 | 75142252 | + | 1 | boxD 1n |
| 2 | SNORD46 | m6A_site_4620 | chr1 | 45242258 | + | 4 | boxD 1n |
| | SNORD46 | m6A_site_122222 | chr7 | 132437879 | + | 2 | boxD 1n |
| 3 | SNORD48 | m6A_site_111371 | chr6 | 31803100 | + | 4 | boxD 1n |
| 4 | SNORD101 | m6A_site_115173 | chr6 | 133136512 | + | 1 | boxD 1n |
| 5 | SNORD5 | m6A_site_25652 | chr11 | 93466398 | – | 2 | boxD 1n |
| 6 | SNORD67 | m6A_site_22376 | chr11 | 46783944 | – | 3 | boxD 1n |
| 7 | SNORD71 | m6A_site_50014 | chr16 | 71792313 | – | 2 | boxD 1n |
| 8 | SNORD89 | m6A_site_74416 | chr2 | 101889404 | – | 1 | boxD 1n |
| 9 | SNORD2 | m6A_site_95922 | chr3 | 186502617 | + | 1 | boxD' 1n |
| 10 | SNORD29 | m6A_site_23425 | chr11 | 62621408 | – | 1 | boxD' 1n |
| 11 | SNORD41 | m6A_site_64597 | chr19 | 12817310 | – | 1 | boxD' 1n |
| 12 | SNORD44 | m6A_site_10668 | chr1 | 173835140 | – | 9 | boxD' 1n |
| 13 | SNORD57 | m6A_site_79190 | chr20 | 2637610 | + | 1 | boxD' 1n |
| 14 | SNORD62A | m6A_site_133909 | chr9 | 134361128 | + | 2 | boxD' 1n |
| | SNORD62B | m6A_site_133912 | chr9 | 134365904 | + | 5 | boxD' 1n |
| Mouse | SNORD2 | m6A_site_29280 | chr16 | 23108986 | + | 1 | boxD' 1n |

the diffraction in most cases. Crystallographic statistics are presented in Materials and Methods.

The first species studied contained N$^6$-methyladenine paired with uridine (PDB 5LR5). This sequence contains GGACU, which is methylated with the highest frequency in cellular RNA [9]. The RNA duplex adopts standard A-form helical geometry and the N$^6$mA-U base pairs are normal Watson–Crick pairs (Fig 5A). Formation of the *cis* Watson–Crick base pair requires that the N$^6$-methyl adopts an *anti* geometry to allow conventional basepairing with H-bonding from AN6 to UO4. These results are in good agreement with recent NMR studies in solution of an RNA duplex from Kool *et al* [43].

We synthesized a second self-complementary RNA strand that would hybridize to form central consecutive G·A pairs flanked by G-C base pairs, with and without a methyl group on the adenine N6. The two species adopted closely similar structures (Fig 5B and C, Appendix Fig S2), with the G·A and G·6mA forming *cis* Watson–Crick base pairs in both cases that are well superimposed, irrespective of the presence of the methyl group on AN6. Like the A-U base pair, the formation of the G·6mA base pair requires the *anti* isomer of the N$^6$-methyladenine. We conclude that N$^6$-methylation of adenine need not lead to disruption of the Watson–Crick G·A pairs.

We studied another duplex of sequence identical to that of the previous one, except that the G-C base pairs flanking the central G·A pairs were replaced by G·U pairs (Fig 5D and E). Two forms were synthesized, with and without N$^6$-methyladenine replacing the central adenine bases that oppose the guanine nucleotides. Both were crystallized, and structures solved for the unmethylated RNA (PDB 5LR3) at 1.65-Å resolution and the methylated RNA (PDB 5LR4) at 1.72 Å (Appendix Fig S2). The unmodified RNA formed a fully basepaired helix, but in contrast to the previous sequence, the G·A pairs formed *trans* sugar-Hoogsteen base pairs with two H-bonds between GN2:AN7 (2.8 Å) and AN6:GN3 (3.4 Å; Fig 5D). This is the same as the two *trans* sugar-Hoogsteen G·A base pairs found in the core of the k-turn. The flanking G·U pairs form *trans* base pairs connected by a single H-bond GN2:UO4 (2.8 Å). In marked contrast, in the N$^6$-methyladenine-containing duplex the guanine and N$^6$-methyladenine do not form base pairs (Fig 5E). Superposition (Fig 6) shows that it is primarily the N$^6$-methyladenine that has become displaced, with a large in-plane translation so that the previously H-bonded distances are now > 6 Å. This avoids a steric clash between the additional methyl groups and the ribose of the opposing guanine (AN6 is just 3 Å from the ribose in the *trans* sugar-Hoogsteen G·A base pair). In its new position, AN6 donates a H-bond to the O2′ of the opposing G (2.8 Å) and the methyl group is free from steric clash.

Thus, the effect of N$^6$-methylation of adenine in this context is the complete disruption of the *trans* sugar-Hoogsteen base pair with guanine and is therefore incompatible with the k-turn conformation. This can be seen if a methyl group is added to the N6 position of A1n in a standard k-turn, whereupon the methyl can be seen to clash with the ribose of G1b (Appendix Fig S3). This provides a structural explanation for the observed failure of the k-turn methylated at the A1n position to bind the 15.5-kDa protein and adopt the k-turn conformation.

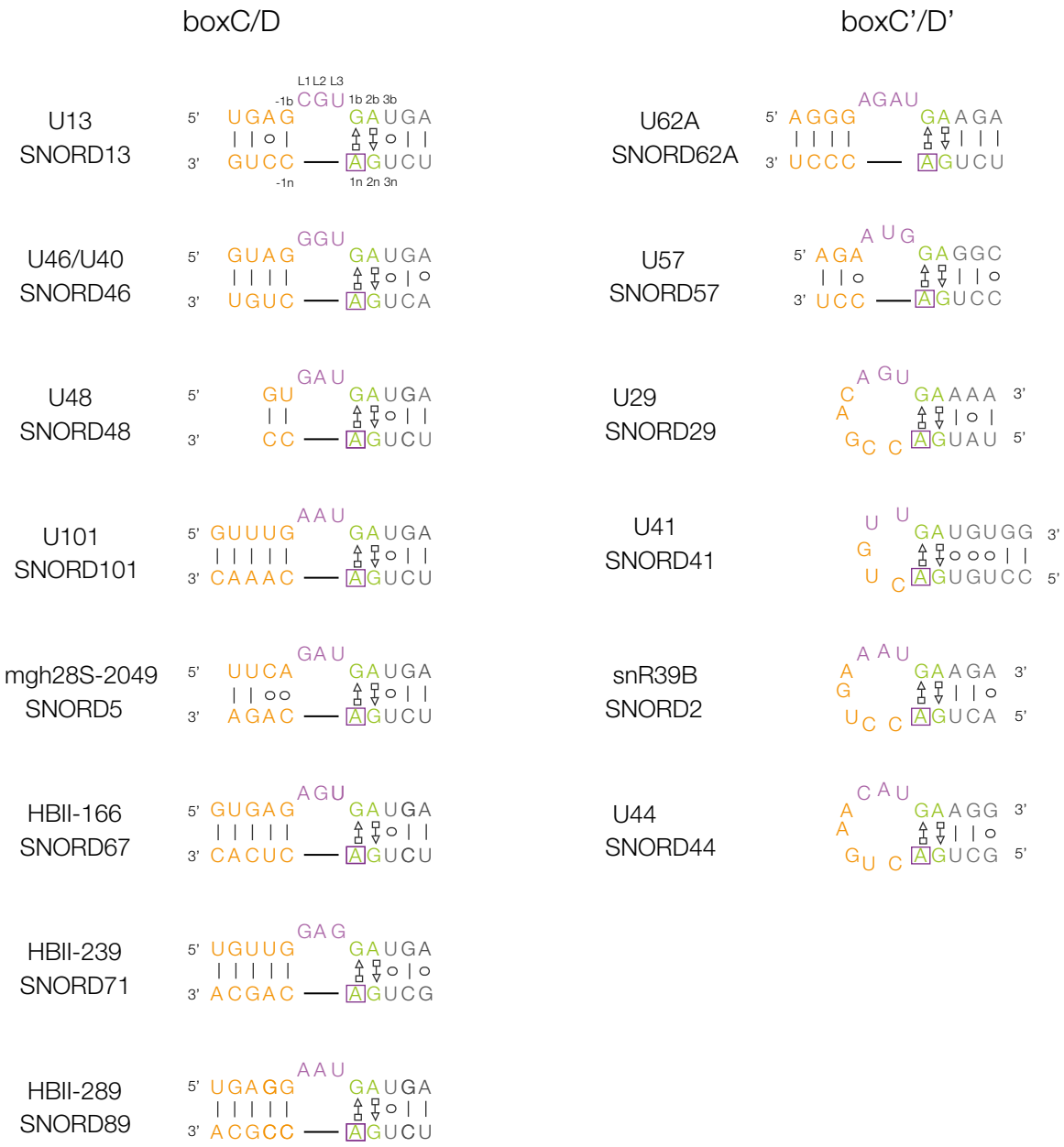


**Figure 3. Human box C/D and C'/D' demonstrated to be methylated *in vivo*.**
In each case, the site of methylation is the A1n shown boxed. Note that the majority of the box C'/D' sequences are k-loop structures.

## Discussion

N$^6$-methyladenine is the most common covalent modification of mRNA in eukaryotes. In principle, there are two ways of expressing N$^6$-methyladenine modification. One is recognition by a specific binding protein, frequently called a "reader" in the language of epigenetics. For example, He and colleagues have identified many Gm$^6$AC sites in RNA that bind the YTHDF2 protein [9,11]. Alternatively, N$^6$-methylation of adenine could alter the local conformation of RNA. We have shown that the Watson–Crick base pairs A-U and A-G can form normally despite methylation of adenine at N6, although the A-U base pair has been shown to be destabilized to some degree [43]. In marked contrast, we have found that the *trans* Hoogsteen-sugar A·G pair is completely disrupted by inclusion of N$^6$-methyladenine. This base pair is frequently found in RNA structures that are not regular duplex, and form the core of the k-turn structure where the conserved adenine bases make key cross-strand hydrogen bonds. We have shown here that this provides the basis for a probable regulatory mechanism for box C/D snoRNP assembly. The 15.5k protein fails to bind to the k-turn when the A1n is methylated at the exocyclic N6. All the specific interactions between this class of protein and k-turns are made with the conserved guanine nucleotides at the 1b and 2n positions that lie in the major groove on

 

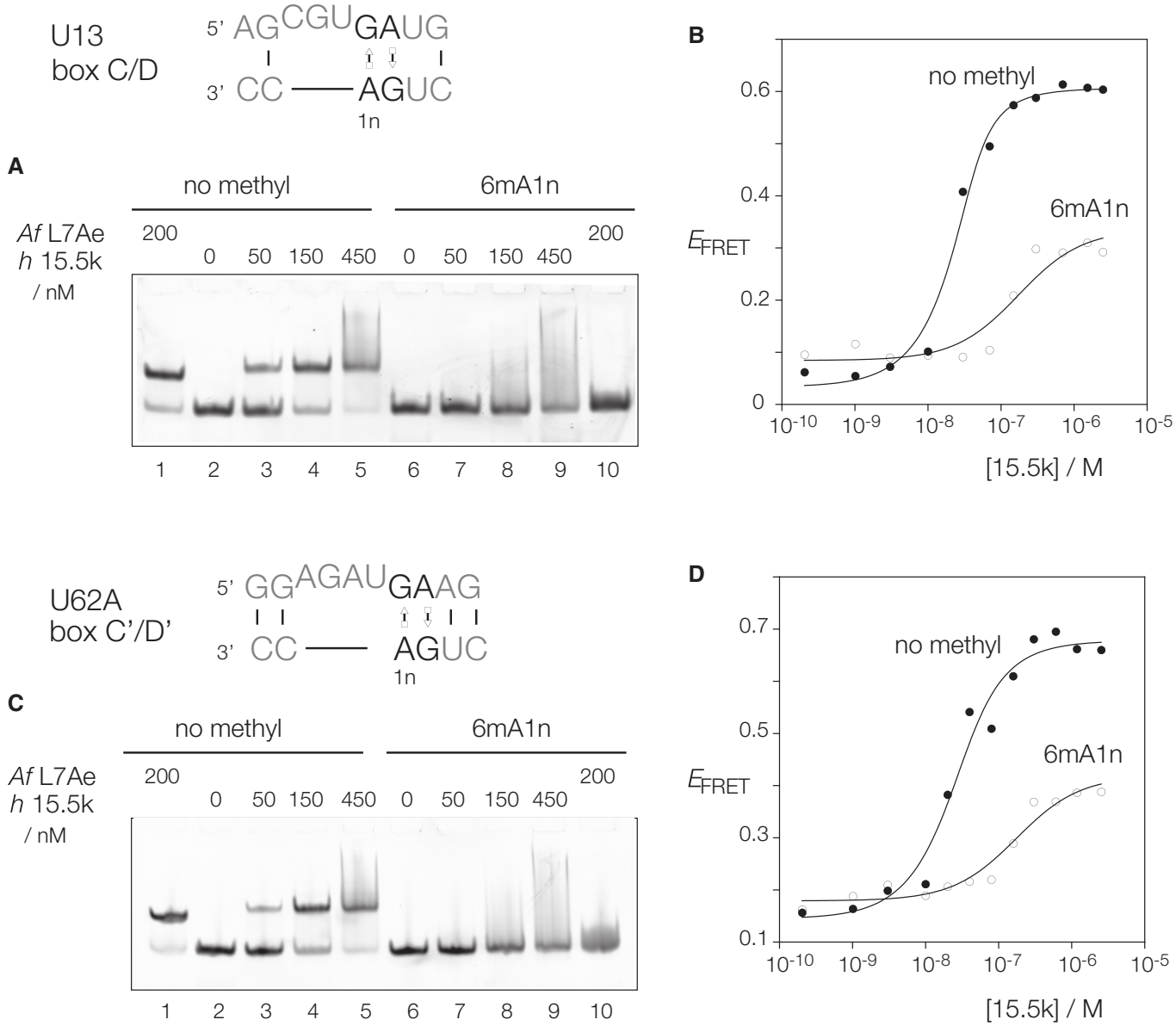


**Figure 4. 15.5-kDa protein binding and induced folding of k-turn conformation is blocked by N$^6$-methylation of adenine in box C/D and C'/D' snoRNA.**

A–D Two human snoRNA k-turns with -1n = C (thus creating a GAC methylation target on the non-bulged strand) have been chosen as examples. Human 15.5k protein binding was studied by gel electrophoretic retardation analysis (A and C) and induced folding analyzed by FRET between fluorescein and Cy3 terminally attached to a short duplex (B and D). The chosen snoRNA species were the SNORD13 (U13) box C/D (A, B) and SNORD62A (U62A) box C'/D' (C, D) k-turns. Each species was studied with and without N$^6$-methylation at the A1n position. 200 nM RNA was incubated with the indicated concentration of 15.5k, or *A. fulgidus* L7Ae proteins and applied to 10% polyacrylamide gels electrophoresed under non-denaturing conditions (A and C). Binding of either protein to the unmodified RNA (tracks 1 through 5) led to the formation of discrete retarded species. At higher concentrations of 15.5k, a continuous smear of complexes ran up the gel suggesting non-specific binding beyond stoichiometric conditions. By contrast, no specific RNA–protein complexes were observed when N$^6$-methyladenine-containing RNA was used (tracks 6 through 10). FRET efficiency ($E_{FRET}$) was measured as a function of 15.5k concentration for non-methylated RNA (closed circles) and N$^6$-methyladenine-containing RNA (open circles). The data have been fitted to a simple binding model (line).

the outside of the kinked RNA, whereas the A1n is on the inside of the structure making no contact with the protein [35]. This class of protein therefore makes indirect recognition of the methylation, resulting from the overall RNA structure rather than specific contacts. Recently, it has been shown that RNA structure can be affected *in vitro* by N$^1$-methylation of A or G [44], but we have not found evidence for such modification occurring naturally in box C/D snoRNA sequences.

The great majority of known k-turn-forming sequences have a C-G base pair in the -1b, -1n position, so creating a GAG sequence on the unbulged strand that is not a target for N$^6$-methylation at A1n. This is true for almost all the known ribosomal and riboswitch

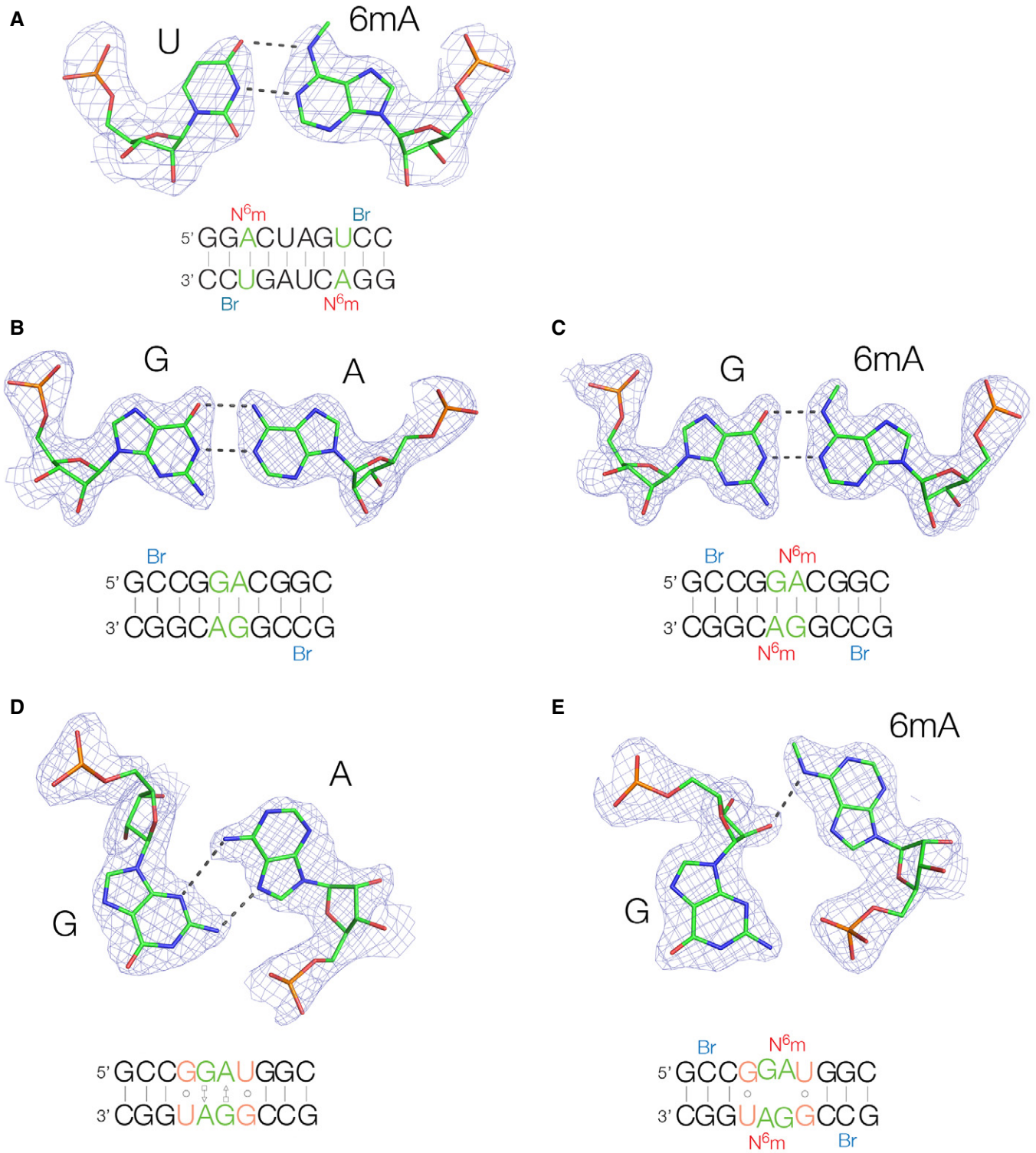


**Figure 5.**

k-turn sequences. However, we have shown here that in a subset of human box C/D and C'/D' snoRNA the -1b,-1n base pair is reversed so placing a C at the -1n position, and thereby creating a GAC sequence that potentially targets the A1n for N$^6$-methylation. Approximately half of these have been shown (generally in multiple experiments) to be methylated *in vivo*. Importantly, the -1n = C is strongly conserved for those that are methylated, whereas this is not true for those that are not methylated.

We have shown here that N$^6$-methylation of A1n in human box C/D and C'/D' k-turns known to undergo methylation *in vivo*

 

**Figure 5. Crystal structures of duplex RNA containing base pairs involving adenine or N$^6$-methyladenine.**
In each case, the relevant base pair is shown with its $2F_O$-$F_C$ map contoured at 1.2σ. The sequences of each self-complementary duplex are shown, with the relevant base pair highlighted in green, and N$^6$-methyl modification in red. 5-Bromocytosine nucleotides are shown blue; each structure was solved by SAD using the anomalous scatter from the two bromine atoms, except for 5LR3 that was determined by soaking with $CuCl_2$.

A A duplex containing a N$^6$-methyladenine-uracil base pair (PDB 5LR5). Crystals of space group $P6_5$ were obtained that diffracted to 2.27 Å. A standard *cis* Watson–Crick base pair is formed in this duplex, despite the presence of the N$^6$-methyl group.

B, C Accommodation of N$^6$-methyladenine in a *cis* Watson–Crick G·A base pair. Two duplex species were constructed containing adjacent G·A base pairs flanked by G-C base pairs, with (B, PDB 5LQO) and without (C, PDB 5LQT) N$^6$-methyladenine at 1.87 and 1.50-Å resolution, respectively. In both structures, the G·A base pairs are *cis* Watson–Crick pairs connected by two hydrogen bonds. Thus, N$^6$-methylation of adenine does not lead to disruption of these Watson–Crick G·A pairs.

D, E Disruption of a *trans* sugar-Hoogsteen G·A base pair by N$^6$-methyladenine. Crystal structures of RNA duplexes in which guanine opposes adenine or N$^6$-methyladenine with flanking G·U base pairs. In the absence of the N$^6$-methyl group (D, PDB 5LR3 at 1.65-Å resolution), a *trans* Hoogsteen-sugar G·A base pair is formed. In marked contrast, the N$^6$-methyladenine does not form a base pair with the guanine (E, PDB 5LR4 at 1.72-Å resolution), and there is no hydrogen bonding between the two nucleobases. Thus, N$^6$-methylation of adenine prevents the formation of the *trans* Hoogsteen-sugar G·A base pair.

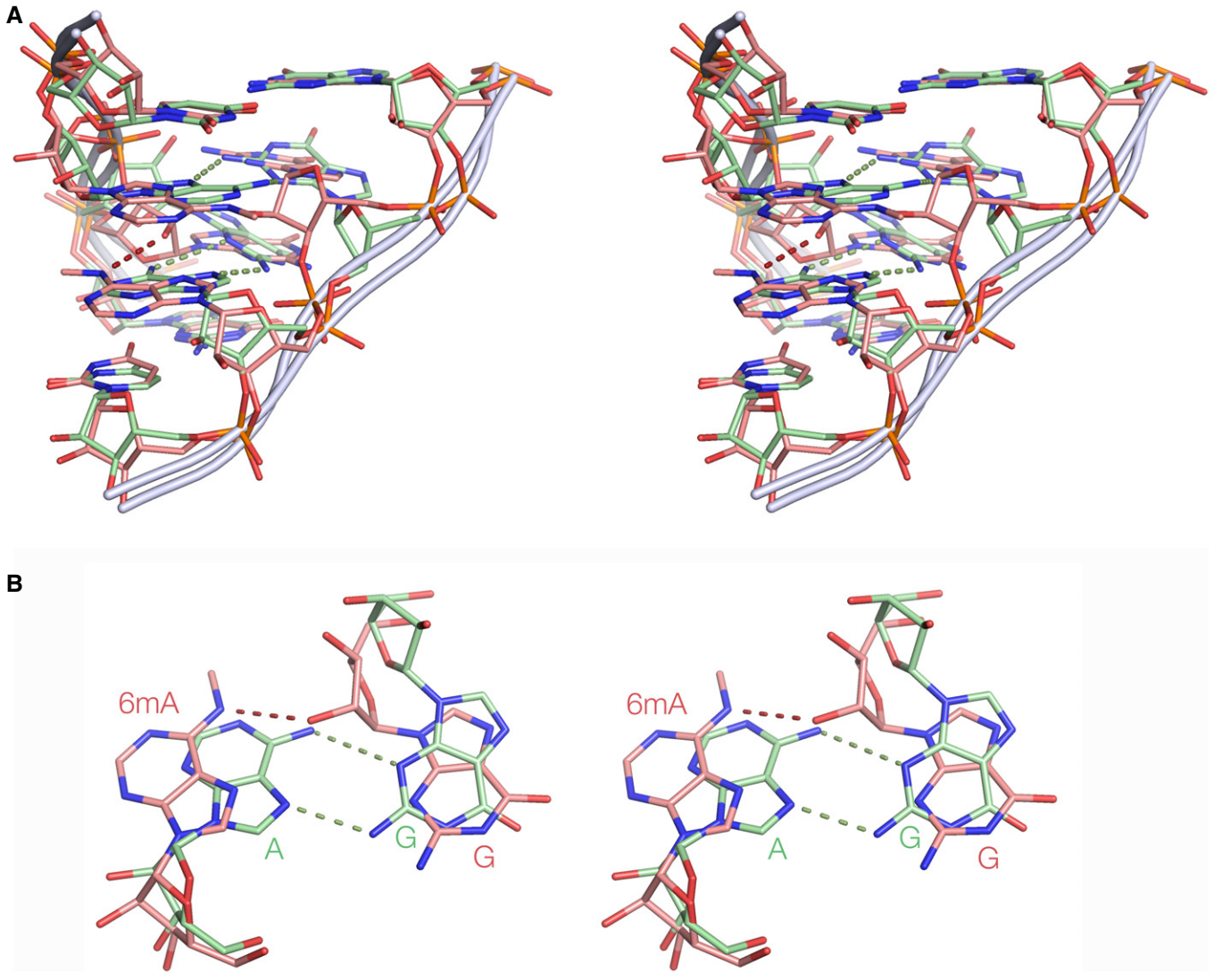


**Figure 6. Superposition of RNA helices with potential *trans* sugar-Hoogsteen G·A pairs (PDB 5LR3 and 5LR4), with and without N$^6$-methylation of adenine.**
The unmethylated structure is shown (green) and the methylated structure (pink). Images are shown as parallel-eye stereoscopic pairs.

A Stereo image of superimposed structures, showing the central G·A pairs and flanking G-U base pairs.

B Superimposed view of one of the G·A pairs. Note that the G·N$^6$mA base pair is disrupted, such that the N$^6$-methyladenine is significantly translated away from the opposing guanine base. The RMSD for the four G, A nucleotides is 0.962 Å.

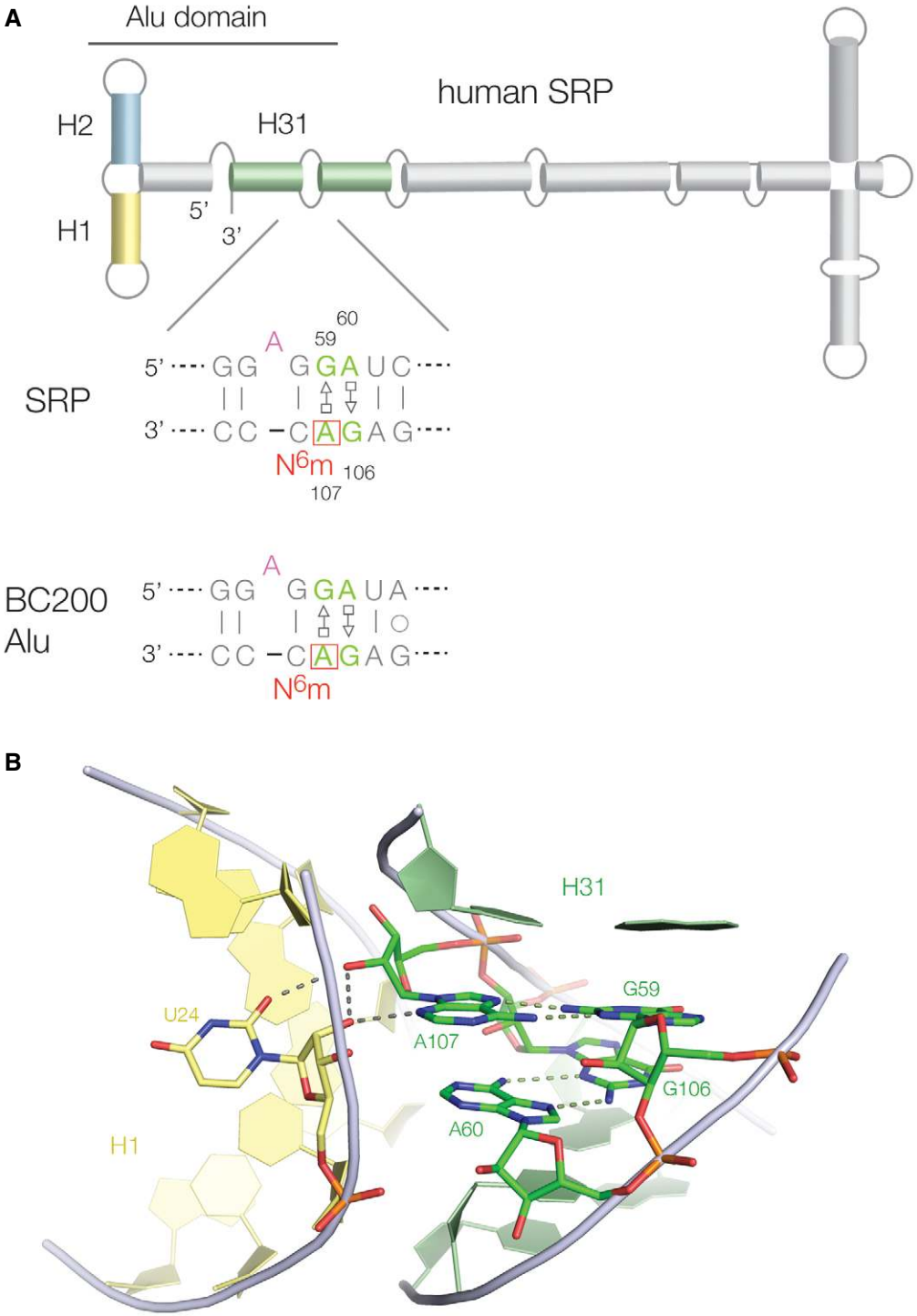


**Figure 7. N$^6$-methylation of an adenine in human SRP, at a *trans* Hoogsteen-sugar A·G base pair that mediates a tertiary contact.**

A A schematic showing the secondary structure of human SRP. Below is shown methylated sequence, and its equivalent in the Alu element BC200. Both have been shown to be N$^6$-methylated at the adenine boxed in red.

B The tertiary contact between helices 31 (green, containing the A·G pairs) and helix 1 (yellow) in the Alu domain of SRP, PDB 5AOX [58]. The A·G pairs both form *trans* Hoogsteen-sugar base pairs with the adenine bases directed into the minor groove of the H1 helix. A107 makes hydrogen bonding contacts between the two helices.

prevent the binding of the 15.5k protein and the concomitant folding of the k-turn into the kinked conformation. This is the first stage of the assembly of the box C/D snoRNP, without which formation of an active methylation complex cannot proceed further [30]. Although assembly factors are also involved [32,45–47], the initial binding of 15.5k protein is fundamental, and blocking the required

 

RNA structure is likely to be fatal to the assembly regardless. Thus, the assembly of these box C/D snoRNPs could plausibly be regulated by N$^6$mA methylation of the guide RNA species. It has been shown that binding 15.5k protein stabilizes box C/D snoRNA [48], and if complex formation fails to occur, the RNA is unstable to degradation [49]. In the absence of any of the core, snoRNP proteins box C/D snoRNA failed to accumulate in the nucleolar body of the nucleolus [50].

Is this restricted solely to box C/D snoRNA? 15.5k additionally binds the U4/U6.U5 tri-snRNP in spliceosome assembly [51], where it also interacts with a k-turn in the RNA [52] as the first stage of assembly [53]. Given the similarities to box C/D snoRNP assembly, could this be subject to the same kind of regulation? In fact the U4 k-turn sequence is standard with -1n = G, and this is strongly conserved from humans down to yeast. So this cannot be subject to regulation by methylation in the same way as the box C/D snoRNP species.

However, we have found data that are indicative of potential regulation by N$^6$mA methylation at G·A base pairs in other systems. In fact one of the box C/D k-turns we identified as methylated (SNORD71, HBII 239; Fig 3) has been shown to be a precursor of the human microRNA mir768 [54] so connecting this with regulatory RNA species. Searching more widely we noted that the human signal recognition particle (SRP) RNA Alu domain contains a sequence that had been considered as a putative k-turn, with the normal consecutive G·A and A·G base pairs (Fig 7). Moreover, like box C/D snoRNP, the SRP is assembled in the nucleolus [55,56]. This has a $HS_2HS_1$ structure [57], but the known *Haloarcula marismortui* k-turn Kt-58 has the same secondary structure and a closely similar sequence. The nucleotide immediately 3′ of the GA sequence of SRP on the unbulged strand (C108 on the lower strand as drawn in Fig 7) is strongly conserved as cytosine, so creating a potential GAC methylation target. Examination of a recent crystal structure of SRP [58] (Appendix Fig S4B) shows that while this sequence did not adopt k-turn conformation, consecutive *trans* sugar-Hoogsteen G·A and A·G base pairs were formed that directed the adenine nucleobases into the minor groove of the juxtaposed helix 1 to make an A-minor interaction to stabilize the tertiary structure. A107 N3 accepts an H-bond from the O2′ of U24, and its O2′ donates an H-bond to O2 of U24 (Fig 7B). This is closely analogous to the A-minor interactions found in the core of a standard k-turn structure, but in this case, they are making a longer-range tertiary contact. We examined the RMBase database [39] to see whether the central adenine (A107) is methylated *in vivo*. This revealed that this adenine has indeed been demonstrated to N$^6$-methylated in 14 independent experiments (Appendix Fig S4C). A107 would correspond to A1n were this forming a k-turn and is the nucleotide that makes the key cross-helix H-bonds that fixes the tertiary structure (Fig 7B). From our crystallography, we know that N$^6$-methylation is incompatible with the required *trans* sugar-Hoogsteen G·A base pair and that the adenine must translocate substantially. It is therefore most likely that methylation would destabilize the folded structure of the SRP.

Generalizing a little further, the left-hand side of SRP (as depicted in Fig 7A) is closely related to the Alu retrotransposon, which is an extremely widespread human mobile genetic element. We examined one Alu element BC200 using RMBase and discovered that the equivalent adenine is indeed N$^6$-methylated *in vivo* (Appendix Fig S4). We further examined the first 30 human Alu elements (from a total of 1,862 entries) in the RMBase database and found that 11 were methylated at the corresponding adenine (i.e. the position corresponding to A1n in the k-turn) (Appendix Fig S4C). Evidently, this adenine is subject to N$^6$-methylation at a high frequency in Alu elements in human cells.

In summary, crystallographic investigation shows that the major structural effect of N$^6$-methylation of adenine is likely to be manifest through the *trans* sugar-Hoogsteen G·A sheared base pair rather than Watson–Crick base pairs. These are widely used in RNA structures, including rather prominently in k-turns. We find that a subset of box C/D snoRNAs are methylated at the 1n position and that this blocks both 15.5k binding and the formation of the kinked conformation *in vivo*. But these effects are not restricted to k-turns, and can apply to any structure that uses *trans* sugar-Hoogsteen G·A base pairs, and we have found equivalent N$^6$-methylation of adenine in human SRP and in related Alu elements. It is likely that control of RNA conformation by N$^6$-methylation of adenine in G·A base pairs is quite general.

## Materials and Methods

### Bioinformatic analysis

#### *Human box C/D k-turn WebLogo*

A full alignment of 262 of human box C/D sequences taken from snoRNABase [37] (https://www-snorna.biotoul.fr//) was made using Jalview (Jalview 2.9) [59]. The k-turn region was aligned manually based on the known pattern of conserved nucleotides. A WebLogo plot [60] showing the occurrence of box C/D sequences in human snoRNA was made using the website http://weblogo.threeplusone.com.

#### *Identification of box C/D RNAs with a 2n = G, 1n = A, and -1n = C sequence*

Human box C/D sequences extracted from snoRNABase [37] and snOPY [38] databases (http://snoopy.med.miyazaki-u.ac.jp) were checked with the Microsoft Word *search* function and visual alignment to identify box C/D RNAs with 2n = G, 1n = A, and -1n = C sequence.

#### *-1nC conservation analysis*

Box C/D sequences extracted from snoRNABase [37] and snOPY [38] databases were further aligned and manually inspected by Genedoc [61] and Jalview [59]. Jalview was used to calculate the number and percentage of -1n = C. The quality of the alignment was also checked by comparison with a recent alignment of box C/D sequences deposited on Rfam [62,63].

#### *Identification of sites of N$^6$-adenine methylation using RMBase*

Candidate box C/D snoRNAs were used to search RMBase [39] http://mirlab.sysu.edu.cn/rmbase/index.php in order to discover their A1n methylation status.

### RNA synthesis

RNA oligonucleotides were synthesized using *t*-BDMS phosphoramidite chemistry [64] as described in Wilson *et al* [65],

implemented on an Applied Biosystems 394DNA/RNA synthesizer. RNA was synthesized using ribonucleotide phosphoramidites with 2′O-*tert*-butyldimethyl-silyl (*t*-BDMS) protection [66,67] (Link Technologies). *t*-BDMS-protected N$^6$-methyl-A-CE phosphoramidite was obtained from Glen Research. Fluorescein (Link Technologies) and Cy3 (GE Healthcare) were attached to the 5′ termini of the oligonucleotides as phosphoramidites in the final cycle of synthesis as required. Unmodified RNA was deprotected in a 25% ethanol/ammonia solution at room temperature for 3 h and evaporated to dryness. Oligonucleotides containing N$^6$-methyladenine were further deprotected for 2 h at 65°C. Oligonucleotides containing 5-bromocytidine (ChemGenes) were deprotected for 36 h at 20°C. All oligoribonucleotides were redissolved in 115 μl of anhydrous DMSO, 60 μl triethylamine (Aldrich), and 75 μl triethylamine trihydrofluoride (Aldrich) to remove *t*-BDMS groups, and agitated at 65°C in the dark for 2.5 h. After cooling on ice for 10 min, 250 μl RNA quenching buffer (Glen Research) was added to stop the reaction, and the oligonucleotides were desalted using NAP-10 columns (GE Healthcare).

RNA for crystallization was purified by gel electrophoresis in polyacrylamide under denaturing conditions in the presence of 7 M urea. The full-length RNA product was visualized by UV shadowing. The band was excised and electroeluted using an Elutrap Electroelution System (GE Healthcare) into 45 mM Tris-borate (pH 8.5), 5 mM EDTA buffer for 8 h at 200 V at 4°C. The RNA was precipitated with ethanol, washed once with 70% ethanol, and suspended in water.

Fluorophore-labeled oligoribonucleotides were purified by gel electrophoresis under denaturing conditions (as described below) and subjected to further purification by reversed-phase HPLC on a C18 column (ACE 10-300, Advanced Chromatography Technologies), using an acetonitrile gradient with an aqueous phase of 100 mM triethylammonium acetate (pH 7.0). Duplex species used for FRET experiments were prepared by mixing equimolar quantities of the appropriate oligoribonucleotides and annealing them in 90 mM Tris-borate (pH 8.5), 10 mM EDTA, 25 mM NaCl, by slow cooling from 90°C to 4°C. They were purified by electrophoresis in 12% polyacrylamide under nondenaturing conditions and recovered by electroelution, followed by ethanol precipitation.

#### Preparation of proteins

##### *L7Ae protein*

*Archeoglobus fulgidus* L7Ae protein was expressed and purified as previously published [35].

##### *15.5-kDa protein*

Human 15.5k protein was expressed as an N-terminal GST fusion in *Escherichia coli* BL21 (DE3) pLysS induced with 0.2 mM isopropyl β-D-1-thiogalactopyranoside at 22°C. Harvested cells were resuspended in PBS buffer and lysed by sonication. Insoluble protein was removed by ultracentrifugation at 45,000 *g* for 60 min at 4°C. The solution was then applied to Glutathione Sepharose 4B resin (GE Healthcare) equilibrated in buffer PBS. The GST tag was cleaved by incubation with 40 U/mg thrombin in 20 mM Tris–HCl (pH 8.0), 50 mM NaCl for 8 h at 25°C. In order to remove contaminating RNA the protein was applied to a heparin column (GE Healthcare) in 20 mM Tris–HCl (pH 8.0) with a 50–2,000 mM NaCl gradient; 15.5k protein eluted at 500 mM NaCl. The purified protein was concentrated to 10 mg/ml.

#### FRET analysis of k-turn folding

Fluorescence resonance energy transfer efficiency was measured from duplex RNA terminally 5′-labeled with fluorescein and Cy3. RNA duplexes contained a central box C/D sequence or N$^6$-A1n-substituted variant (from position −2 to 4). The sequences used were (written 5′–3′):

U13top: F –CCAGUCAGUGAGCGUGAUGCAUGUCAGG
U62Atop: F –CCAGUCAGUGGGAGAUGAAGCAUGUCAGG
U48top: F –CCAGUCAGUGGUGAUGAUGCAUGUCAGG
lower strand: Cy3-CCUGACAUGCUGACCCACUGACUGG

Note that the lower strand is the same in each case.

Absorption spectra were measured in 90 mM Tris-borate (pH 8.3) in a 5-mm path-length cuvette in 2 μl volumes using a NanoDrop 2000c spectrophotometer (Thermo Scientific). Spectra were deconvoluted using a corresponding RNA species labeled only with Cy3, and fluorophore absorption ratios calculated using a MATLAB program. Fluorescence spectra were recorded in 90 mM Tris-borate (pH 8.3) at 4°C using an SLM-Aminco 8100 fluorimeter. Spectra were corrected for lamp fluctuations and instrumental variations, and polarization artifacts were avoided by setting excitation and emission polarizers crossed at 54.7°. Values of FRET efficiency ($E_{\mathrm{FRET}}$) were measured using the acceptor normalization method [68] implemented in MATLAB.

$E_{\mathrm{FRET}}$ as a function of 15.5k protein concentration was fitted to:

$$E_{\mathrm{FRET}} = E_0 + \Delta E_{\mathrm{FRET}} \cdot \frac{(1 + K_A P_T + K_A R_T) - \sqrt{(1 + K_A P_T + K_A R_T)^2 - 4 R_T K_A^2 P_T}}{2 R_T K_A} \quad (1)$$

where $E_0$ is the initial FRET efficiency in the absence of added protein, $\Delta E_{\mathrm{FRET}}$ is the full range of the change in FRET efficiency, $K_A$ is the apparent association constant, and $P_T$ and $R_T$ are the total concentration of 15.5k and RNA, respectively.

#### Electrophoretic analysis of protein binding to snoRNA k-turns

Binding of recombinant 15.5k and AfL7Ae protein to the U13 and U62A k-turn motif RNA was analyzed by gel electrophoresis. 200 nM Cy3-labeled RNA (the same species as used in the FRET experiments, see above) was incubated in 45 mM Tris-borate (pH 8.3) with various concentrations of proteins (15.5k or AfL7Ae) in a final volume of 10 μl at 7°C for 60 min. An equal volume of loading buffer containing 10% glycerol and 45 mM Tris-borate (pH 8.3) was added to the reactions, which were then electrophoresed in 10% native polyacrylamide gels in 45 mM Tris-borate (pH 8.3) at 20 V/cm at 7°C for 1 h. Fluorescent RNA was visualized using a Typhoon 9500 fluorimager (GE Healthcare).

#### Isothermal titration calorimetry

Titrations were performed at 298 K using an ITC-200 microcalorimeter (GE). RNA solutions were prepared by diluting concentrated stocks into the binding buffer containing 40 mM HEPES (pH 7.5),

 

100 mM KCl, 10 mM $MgCl_2$ to a final concentration of 20 μM. 15.5k was prepared in the same binding buffer with a concentration of 200 μM. Solutions were degassed for 2–5 min before loading. The sample cell was filled with 200 μl of RNA. 15.5k protein was injected into the RNA solution, using 0.4 μl for the first injection and 2 μl for the subsequent 19 injections using a computer-controlled 40-μl microsyringe with an injection interval of 120 s. Titration of protein into the binding buffer or titration of the binding buffer into the RNA solution produced negligible heat evolution. Integrated heat data were analyzed using a one-set-of-sites model in MicroCal Origin following the manufacturer's instructions. The first data point was excluded in the analysis. The binding parameters $\Delta H$ (cal mol$^{-1}$), $K$ (M$^{-1}$) and $n$ (moles of 15.5k bound per RNA) were fitted. The binding free energy $\Delta G$ and reaction entropy $\Delta S$ were calculated using the relationships $\Delta G = -RT\ln K$ ($R$ = 1.9872 cal mol$^{-1}$ K$^{-1}$, $T$ = 298 K) and $\Delta G = \Delta H - T\Delta S$. The dissociation constant $K_d$ was calculated as $1/K$.

#### Crystallization, structure determination, and refinement

The sequences are shown in Fig 4. All RNA used in crystallization in this study was formed by hybridization of self-complementary strands. A solution of 1 mM RNA in 5 mM Tris–HCl (pH 8.0), 100 mM NaCl was heated to 95°C for 1 min. The solution was slowly cooled to 20°C, and $MgCl_2$ was added to a final concentration of 10 mM. The complete conditions used for crystallization of each species are given in Appendix Table S3.

All data were collected on beamline I02 of Diamond Light Source (Harwell, UK), and processed by XIA2 version 0.4.0.0 [69]. The resolution cutoff for the data was determined by examining by $CC_{1/2}$ and density map as described previously [70].

All the structures' initial phases were acquired from the SAD data by locating the bromine atoms with Autosol in the PHENIX suite, except for 5LR3 that was determined by soaking with $CuCl_2$. Models were adjusted manually using Coot [71] and subjected to several rounds of adjustment and optimization using Coot, phenix.refine and PDB_REDO [72]. Model geometry and the fit to electron-density maps were monitored with MOLPROBITY [73] and the validation tools in Coot. Data collection and refinement statistics are presented in Appendix Table S4.

#### Data availability and accession numbers

Coordinates of the crystal structures described in this work are deposited with the PDB with accession numbers 5LR5, 5LQO, 5LQT, 5LR3, and 5LR4.

**Expanded View** for this article is available online.

### Acknowledgements
We thank our colleague Dr. Tim Wilson for discussion and Dr. Alessio Ciuili for use of the calorimeter. This study was supported by Cancer Research UK (CRUK) program grant A18604.

### Author contributions
LH performed bioinformatic analysis and crystallography, SA carried out RNA synthesis, JW performed bioinformatic analysis, and LH and DMJL planned experiments, analyzed data and wrote the paper.

### Conflict of interest
The authors declare that they have no conflict of interest.

## References

1. He C (2010) Grand challenge commentary: RNA epigenetics? *Nat Chem Biol* 6: 863 – 865
2. Cantara WA, Crain PF, Rozenski J, McCloskey JA, Harris KA, Zhang X, Vendeix FA, Fabris D, Agris PF (2011) The RNA Modification Database, RNAMDB: 2011 update. *Nucleic Acids Res* 39: D195 – D201
3. Schibler U, Kelley DE, Perry RP (1977) Comparison of methylated sequences in messenger RNA and heterogeneous nuclear RNA from mouse L cells. *J Mol Biol* 115: 695 – 714
4. Dominissini D, Moshitch-Moshkovitz S, Schwartz S, Salmon-Divon M, Ungar L, Osenberg S, Cesarkas K, Jacob-Hirsch J, Amariglio N, Kupiec M *et al* (2012) Topology of the human and mouse m6A RNA methylomes revealed by m6A-seq. *Nature* 485: 201 – 206
5. Meyer KD, Saletore Y, Zumbo P, Elemento O, Mason CE, Jaffrey SR (2012) Comprehensive analysis of mRNA methylation reveals enrichment in 3' UTRs and near stop codons. *Cell* 149: 1635 – 1646
6. Liu N, Parisien M, Dai Q, Zheng G, He C, Pan T (2013) Probing N6-methyladenosine RNA modification status at single nucleotide resolution in mRNA and long noncoding RNA. *RNA* 19: 1848 – 1856
7. Zhou KI, Parisien M, Dai Q, Liu N, Diatchenko L, Sachleben JR, Pan T (2016) N(6)-Methyladenosine Modification in a Long Noncoding RNA Hairpin Predisposes Its Conformation to Protein Binding. *J Mol Biol* 428: 822 – 833
8. Beemon K, Keith J (1977) Localization of N6-methyladenosine in the Rous sarcoma virus genome. *J Mol Biol* 113: 165 – 179
9. Wang X, Lu Z, Gomez A, Hon GC, Yue Y, Han D, Fu Y, Parisien M, Dai Q, Jia G *et al* (2014) N6-methyladenosine-dependent regulation of messenger RNA stability. *Nature* 505: 117 – 120
10. Meyer KD, Patil DP, Zhou J, Zinoviev A, Skabkin MA, Elemento O, Pestova TV, Qian SB, Jaffrey SR (2015) 5' UTR m(6)A Promotes Cap-Independent Translation. *Cell* 163: 999 – 1010
11. Wang X, Zhao BS, Roundtree IA, Lu Z, Han D, Ma H, Weng X, Chen K, Shi H, He C (2015) N6-methyladenosine modulates messenger RNA translation efficiency. *Cell* 161: 1388 – 1399
12. Wang Y, Li Y, Toth JI, Petroski MD, Zhang Z, Zhao JC (2014) N6-methyladenosine modification destabilizes developmental regulators in embryonic stem cells. *Nat Cell Biol* 16: 191 – 198
13. Bokar JA, Shambaugh ME, Polayes D, Matera AG, Rottman FM (1997) Purification and cDNA cloning of the AdoMet-binding subunit of the human mRNA (N6-adenosine)-methyltransferase. *RNA* 3: 1233 – 1247
14. Jia G, Fu Y, Zhao X, Dai Q, Zheng G, Yang Y, Yi C, Lindahl T, Pan T, Yang YG *et al* (2011) N6-methyladenosine in nuclear RNA is a major substrate of the obesity-associated FTO. *Nat Chem Biol* 7: 885 – 887
15. Zheng G, Dahl JA, Niu Y, Fedorcsak P, Huang CM, Li CJ, Vagbo CB, Shi Y, Wang WL, Song SH *et al* (2013) ALKBH5 is a mammalian RNA demethylase that impacts RNA metabolism and mouse fertility. *Mol Cell* 49: 18 – 29
16. Gerken T, Girard CA, Tung YC, Webby CJ, Saudek V, Hewitson KS, Yeo GS, McDonough MA, Cunliffe S, McNeill LA *et al* (2007) The obesity-associated FTO gene encodes a 2-oxoglutarate-dependent nucleic acid demethylase. *Science* 318: 1469 – 1472

 

17. Fischer J, Koch L, Emmerling C, Vierkotten J, Peters T, Bruning JC, Ruther U (2009) Inactivation of the Fto gene protects from obesity. *Nature* 458: 894 – 898
18. Zhao X, Yang Y, Sun BF, Shi Y, Yang X, Xiao W, Hao YJ, Ping XL, Chen YS, Wang WJ *et al* (2014) FTO-dependent demethylation of N6-methyladenosine regulates mRNA splicing and is required for adipogenesis. *Cell Res* 24: 1403 – 1419
19. Kiss-Laszlo Z, Henry Y, Bachellerie JP, Caizergues-Ferrer M, Kiss T (1996) Site-specific ribose methylation of preribosomal RNA: a novel function for small nucleolar RNAs. *Cell* 85: 1077 – 1088
20. Tycowski KT, Smith CM, Shu MD, Steitz JA (1996) A small nucleolar RNA requirement for site-specific ribose methylation of rRNA in Xenopus. *Proc Natl Acad Sci USA* 93: 14480 – 14485
21. Watkins NJ, Segault V, Charpentier B, Nottrott S, Fabrizio P, Bachi A, Wilm M, Rosbash M, Branlant C, Luhrmann R (2000) A common core RNP structure shared between the small nucleolar box C/D RNPs and the spliceosomal U4 snRNP. *Cell* 103: 457 – 466
22. Tran EJ, Zhang X, Maxwell ES (2003) Efficient RNA 2'-O-methylation requires juxtaposed and symmetrically assembled archaeal box C/D and C'/D' RNPs. *EMBO J* 22: 3930 – 3940
23. Bleichert F, Gagnon KT, Brown BA, Maxwell ES, Leschziner AE, Unger VM, Baserga SJ (2009) A dimeric structure for archaeal box C/D small ribonucleoproteins. *Science* 325: 1384 – 1387
24. Ye K, Jia R, Lin J, Ju M, Peng J, Xu A, Zhang L (2009) Structural organization of box C/D RNA-guided RNA methyltransferase. *Proc Natl Acad Sci USA* 106: 13808 – 13813
25. Xue S, Wang R, Yang F, Terns RM, Terns MP, Zhang X, Maxwell ES, Li H (2010) Structural basis for substrate placement by an archaeal box C/D ribonucleoprotein particle. *Mol Cell* 39: 939 – 949
26. Lin J, Lai S, Jia R, Xu A, Zhang L, Lu J, Ye K (2011) Structural basis for site-specific ribose methylation by box C/D RNA protein complexes. *Nature* 469: 559 – 563
27. Huang L, Lilley DMJ (2016) The kink turn, a key architectural element in RNA structure. *J Mol Biol* 428: 790 – 801
28. Watkins NJ, Newman DR, Kuhn JF, Maxwell ES (1998) *In vitro* assembly of the mouse U14 snoRNP core complex and identification of a 65-kDa box C/D-binding protein. *RNA* 4: 582 – 593
29. Omer AD, Ziesche S, Ebhardt H, Dennis PP (2002) *In vitro* reconstitution and activity of a C/D box methylation guide ribonucleoprotein complex. *Proc Natl Acad Sci USA* 99: 5289 – 5294
30. Watkins NJ, Dickmanns A, Luhrmann R (2002) Conserved stem II of the box C/D motif is essential for nucleolar localization and is required, along with the 15.5K protein, for the hierarchical assembly of the box C/D snoRNP. *Mol Cell Biol* 22: 8342 – 8352
31. Schultz A, Nottrott S, Watkins NJ, Luhrmann R (2006) Protein-protein and protein-RNA contacts both contribute to the 15.5K-mediated assembly of the U4/U6 snRNP and the box C/D snoRNPs. *Mol Cell Biol* 26: 5146 – 5154
32. McKeegan KS, Debieux CM, Boulon S, Bertrand E, Watkins NJ (2007) A dynamic scaffold of pre-snoRNP factors facilitates human box C/D snoRNP assembly. *Mol Cell Biol* 27: 6782 – 6793
33. Turner B, Melcher SE, Wilson TJ, Norman DG, Lilley DMJ (2005) Induced fit of RNA on binding the L7Ae protein to the kink-turn motif. *RNA* 11: 1192 – 1200
34. Wang J, Fessl T, Schroeder KT, Ouellet J, Liu Y, Freeman AD, Lilley DMJ (2012) Single-molecule observation of the induction of k-turn RNA structure on binding L7Ae protein. *Biophys J* 103: 2541 – 2548
35. Huang L, Lilley DMJ (2013) The molecular recognition of kink-turn structure by the L7Ae class of proteins. *RNA* 19: 1703 – 1710
36. McPhee SA, Huang L, Lilley DM (2014) A critical base pair in k-turns that confers folding characteristics and correlates with biological function. *Nat Commun* 5: 5127
37. Lestrade L, Weber MJ (2006) snoRNA-LBME-db, a comprehensive database of human H/ACA and C/D box snoRNAs. *Nucleic Acids Res* 34: D158 – D162
38. Yoshihama M, Nakao A, Kenmochi N (2013) snOPY: a small nucleolar RNA orthological gene database. *BMC Res Notes* 6: 426 – 430
39. Sun WJ, Li JH, Liu S, Wu J, Zhou H, Qu LH, Yang JH (2016) RMBase: a resource for decoding the landscape of RNA modifications from high-throughput sequencing data. *Nucleic Acids Res* 44: D259 – D265
40. Chen K, Lu Z, Wang X, Fu Y, Luo GZ, Liu N, Han D, Dominissini D, Dai Q, Pan T *et al* (2015) High-resolution N(6) -methyladenosine (m(6) A) map using photo-crosslinking-assisted m(6) A sequencing. *Angew Chem* 54: 1587 – 1590
41. Linder B, Grozhik AV, Olarerin-George AO, Meydan C, Mason CE, Jaffrey SR (2015) Single-nucleotide-resolution mapping of m6A and m6Am throughout the transcriptome. *Nat Methods* 12: 767 – 772
42. Turner B, Lilley DMJ (2008) The importance of G.A hydrogen bonding in the metal ion- and protein-induced folding of a kink turn RNA. *J Mol Biol* 381: 431 – 442
43. Roost C, Lynch SR, Batista PJ, Qu K, Chang HY, Kool ET (2015) Structure and thermodynamics of N6-methyladenosine in RNA: a spring-loaded base modification. *J Am Chem Soc* 137: 2107 – 2015
44. Zhou H, Kimsey IJ, Nikolova EN, Sathyamoorthy B, Grazioli G, McSally J, Bai T, Wunderlich CH, Kreutz C, Andricioaei I *et al* (2016) m1A and m1G disrupt A-RNA structure through the intrinsic instability of Hoogsteen base pairs. *Nat Struct Mol Biol* 23: 803 – 810
45. Boulon S, Marmier-Gourrier N, Pradet-Balade B, Wurth L, Verheggen C, Jady BE, Rothe B, Pescia C, Robert MC, Kiss T *et al* (2008) The Hsp90 chaperone controls the biogenesis of L7Ae RNPs through conserved machinery. *J Cell Biol* 180: 579 – 595
46. McKeegan KS, Debieux CM, Watkins NJ (2009) Evidence that the AAA+ proteins TIP48 and TIP49 bridge interactions between 15.5K and the related NOP56 and NOP58 proteins during box C/D snoRNP biogenesis. *Mol Cell Biol* 29: 4971 – 4981
47. Rothe B, Back R, Quinternet M, Bizarro J, Robert MC, Blaud M, Romier C, Manival X, Charpentier B, Bertrand E *et al* (2014) Characterization of the interaction between protein Snu13p/15.5K and the Rsa1p/NUFIP factor and demonstration of its functional importance for snoRNP assembly. *Nucleic Acids Res* 42: 2015 – 2036
48. Szewczak LB, DeGregorio SJ, Strobel SA, Steitz JA (2002) Exclusive interaction of the 15.5 kD protein with the terminal box C/D motif of a methylation guide snoRNP. *Chem Biol* 9: 1095 – 1107
49. Caffarelli E, Fatica A, Prislei S, De Gregorio E, Fragapane P, Bozzoni I (1996) Processing of the intron-encoded U16 and U18 snoRNAs: the conserved C and D boxes control both the processing reaction and the stability of the mature snoRNA. *EMBO J* 15: 1121 – 1131
50. Verheggen C, Mouaikel J, Thiry M, Blanchard JM, Tollervey D, Bordonne R, Lafontaine DL, Bertrand E (2001) Box C/D small nucleolar RNA trafficking involves small nucleolar RNP proteins, nucleolar factors and a novel nuclear domain. *EMBO J* 20: 5480 – 5490
51. Nottrott S, Hartmuth K, Fabrizio P, Urlaub H, Vidovic I, Ficner R, Luhrmann R (1999) Functional interaction of a novel 15.5kD [U4/U6.U5] tri-snRNP protein with the 5' stem-loop of U4 snRNA. *EMBO J* 18: 6119 – 6133

 

52. Vidovic I, Nottrott S, Hartmuth K, Luhrmann R, Ficner R (2000) Crystal structure of the spliceosomal 15.5 kD protein bound to a U4 snRNA fragment. *Mol Cell* 6: 1331 – 1342
53. Nottrott S, Urlaub H, Luhrmann R (2002) Hierarchical, clustered protein interactions with U4/U6 snRNA: a biochemical role for U4/U6 proteins. *EMBO J* 21: 5527 – 5538
54. Ono M, Scott MS, Yamada K, Avolio F, Barton GJ, Lamond AI (2011) Identification of human miRNA precursors that resemble box C/D snoRNAs. *Nucleic Acids Res* 39: 3879 – 3891
55. Politz JC, Yarovoi S, Kilroy SM, Gowda K, Zwieb C, Pederson T (2000) Signal recognition particle components in the nucleolus. *Proc Natl Acad Sci USA* 97: 55 – 60
56. Grosshans H, Deinert K, Hurt E, Simos G (2001) Biogenesis of the signal recognition particle (SRP) involves import of SRP proteins into the nucleolus, assembly with the SRP-RNA, and Xpo1p-mediated export. *J Cell Biol* 153: 745 – 762
57. Lilley DMJ, Clegg RM, Diekmann S, Seeman NC, von Kitzing E, Hagerman P (1995) Nomenclature Committee of the International Union of Biochemistry: a nomenclature of junctions and branchpoints in nucleic acids. Recommendations 1994. *Eur J Biochem* 230: 1 – 2
58. Ahl V, Keller H, Schmidt S, Weichenrieder O (2015) Retrotransposition and crystal structure of an Alu RNP in the ribosome-stalling conformation. *Mol Cell* 60: 715 – 727
59. Waterhouse AM, Procter JB, Martin DMA, Clamp M, Barton GJ (2009) Jalview Version 2 - a multiple sequence alignment editor and analysis workbench. *Bioinformatics* 25: 1189 – 1191
60. Crooks GE, Hon G, Chandonia JM, Brenner SE (2004) WebLogo: a sequence logo generator. *Genome Res* 14: 1188 – 1190
61. Nicholas KB, Nicholas HB Jr, Deerfield DW (1997) GeneDoc: analysis and Visualization of Genetic Variation. *Embnew. News* 4: 14
62. Jorjani H, Kehr S, Jedlinski DJ, Gumienny R, Hertel J, Stadler PF, Zavolan M, Gruber AR (2016) An updated human snoRNAome. *Nucleic Acids Res* 44: 5068 – 5082
63. Burge SW, Daub J, Eberhardt R, Tate J, Barquist L, Nawrocki EP, Eddy SR, Gardner PP, Bateman A (2013) Rfam 11.0: 10 years of RNA families. *Nucleic Acids Res* 41: D226 – D232
64. Beaucage SL, Caruthers MH (1981) Deoxynucleoside phosphoramidites - a new class of key intermediates for deoxypolynucleotide synthesis. *Tetrahedron Lett* 22: 1859 – 1862
65. Wilson TJ, Zhao Z-Y, Maxwell K, Kontogiannis L, Lilley DMJ (2001) Importance of specific nucleotides in the folding of the natural form of the hairpin ribozyme. *Biochemistry* 40: 2291 – 2302
66. Hakimelahi GH, Proba ZA, Ogilvie KK (1981) High yield selective 3'-silylation of ribonucleosides. *Tetrahedron let* 22: 5243 – 5246
67. Perreault J-P, Wu T, Cousineau B, Ogilvie KK, Cedergren R (1990) Mixed deoxyribo- and ribooligonucleotides with catalytic activity. *Nature* 344: 565 – 567
68. Clegg RM (1992) Fluorescence resonance energy transfer and nucleic acids. *Meth Enzymol* 211: 353 – 388
69. Winter G (2010) xia2: an expert system for macromolecular crystallography data reduction. *J Appl Cryst* 43: 186 – 190
70. Karplus PA, Diederichs K (2012) Linking crystallographic model and data quality. *Science* 336: 1030 – 1033
71. Emsley P, Lohkamp B, Scott WG, Cowtan K (2010) Features and development of Coot. *Acta Crystallogr D Biol Crystallogr* 66: 486 – 501
72. Joosten RP, Long F, Murshudov GN, Perrakis A (2014) The PDB_REDO server for macromolecular structure model optimization. *IUCrJ* 1: 213 – 220
73. Chen VB, Arendall WB III, Headd JJ, Keedy DA, Immormino RM, Kapral GJ, Murray LW, Richardson JS, Richardson DC (2010) MolProbity: all-atom structure validation for macromolecular crystallography. *Acta Crystallogr D Biol Crystallogr* 66: 12 – 21
74. Moore T, Zhang Y, Fenley MO, Li H (2004) Molecular basis of box C/D RNA-protein Interactions; Cocrystal structure of archaeal L7Ae and a box C/D RNA. *Structure* 12: 807 – 818